

Reaction and ultraslow diffusion on comb structuresYingjie Liang^{1,*}, Trifce Sandev^{2,†} and Ervin Kaminski Lenzi^{3,‡}¹*Key Laboratory of Coastal Disaster and Defence of Ministry of Education, College of Mechanics and Materials, Hohai University, Nanjing, Jiangsu 211100, China*²*Research Center for Computer Science and Information Technologies, Macedonian Academy of Sciences and Arts, Bulevar Krste Misirkov 2, 1000 Skopje, Macedonia;**Institute of Physics & Astronomy, University of Potsdam, D-14776 Potsdam-Golm, Germany;*
*and Institute of Physics, Faculty of Natural Sciences and Mathematics, Saints Cyril and Methodius University, Arhimedova 3, 1000 Skopje, Macedonia*³*Departamento de Física, Universidade Estadual de Ponta Grossa, Avenida Carlos Cavalcanti 4748, 84030-900 Ponta Grossa, Paraná, Brazil*

(Received 21 November 2019; revised manuscript received 14 February 2020; accepted 20 March 2020; published 16 April 2020)

A two-dimensional (2D) comb model is proposed to characterize reaction-ultraslow diffusion of tracers both in backbones (x direction) and side branches (y direction) of the comblike structure with two memory kernels. The memory kernels include Dirac delta, power-law, and logarithmic and inverse Mittag-Leffler (ML) functions, which can also be considered as the structural functions in the time structural derivative. Based on the comb model, ultraslow diffusion on a fractal comb structure is also investigated by considering spatial fractal geometry of the backbone volume. The mean squared displacement (MSD) and the corresponding concentration of the tracers, i.e., the solution of the comb model, are derived for reactive and conservative tracers. For a fractal structure of backbones, the derived MSDs and corresponding solutions depend on the backbone's fractal dimension. The proposed 2D comb model with different kernel functions is feasible to describe ultraslow diffusion in both the backbone and side branches of the comblike structure.

DOI: [10.1103/PhysRevE.101.042119](https://doi.org/10.1103/PhysRevE.101.042119)**I. INTRODUCTION**

Comblike structure, such as in rock, polymer, and spiny dendrite, is widely encountered in real applications [1–5]. Figure 1 gives a schematic diagram of two-dimensional comblike structure. Diffusion processes of conservative and interacting diffusive particles [6] in these comblike structures usually deviate from Brownian motion, i.e., non-Gaussian diffusion, in which the mean squared displacement (MSD) is a nonlinear function of time [7–10]. Anomalous diffusion in the comblike structure, in which the MSD is a power-law function in time, $\langle x^2(t) \rangle \sim t^\alpha$ ($\alpha \neq 1$), has been extensively studied from both the macroscopic partial differential equation models, e.g., the comb model [11–13], and microscopic or mesoscopic models, e.g., the continuous time random walk (CTRW) model [14–16]. The comb model can well exemplify the anomalous diffusion due to geometric constraints, which play a significant role related to the diffusion environment. For a two-dimensional (2D) case [11], the motions of diffusive particles are allowed in the x direction only where y is zero, in which x and y , respectively, represent the backbone and side branches on the comb. The corresponding 2D comb model describes subdiffusion along the backbone with infinite side branches, which has been well employed to describe cancer proliferation [17], transfer in living organisms [18], and diffusion of

ultracold atoms [19]. It should be noted that in recent years some general forms of the comb model have been proposed to characterize diffusion process in more complicated media, such as heterogeneous diffusion in comb structure with a power-law position dependent diffusion coefficient along the backbone [20], linear reaction in spine and nonlinear reaction along dendrites [21], and more general memory kernels [22]. The existing comb models have been an alternative tool to characterize non-Gaussian diffusion in comblike structures.

It is also found that ultraslow diffusion, another class of non-Gaussian diffusion, exists in comb structure, such as the diffusion process in the three-dimensional (3D) cylindrical comb model with infinite side branches along the backbone [23], also in the 3D comb structure with a 2D “kebab lattice” [24]. Compared with anomalous diffusion, the MSD of ultraslow diffusion is not a power-law function of time, but a logarithmic function of time [25] $\langle x^2(t) \rangle \sim \ln^\alpha t$ ($\alpha > 0$), in which the particles diffuse more slowly than in subdiffusion. Note that the mentioned 3D models only capture the ultraslow diffusion in the backbone, but fail to do that in the side branches. To model ultraslow diffusion in both the backbone and side branches, 2D comb models [22] with special memory kernels attract growing attention, such as uniformly and power-law distributed functions with an integral form. In this study we focus on the comb model, which should have potential ability to describe ultraslow diffusion in both the backbone and side branches.

Ultraslow diffusion has been captured in many real experiments [26], such as particles in aging dense colloidal glass, random walks on bundled structures, interacting many-body

*liangyj@hhu.edu.cn

†trifce.sandev@manu.edu.mk

‡eklenzi@uepg.br

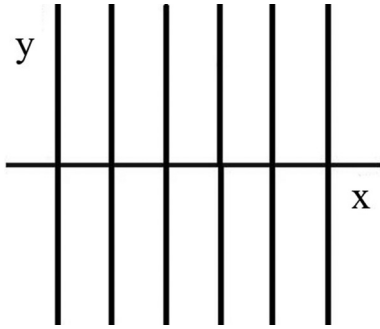


FIG. 1. Schematic diagram of two-dimensional comblike structure, in which x and y , respectively, represent the backbone and side branches of the comb.

systems in low-dimensional disordered environments, and Sinai diffusion in quenched landscapes with a random force field. To model the phenomenon of ultraslow diffusion in heterogeneous media, except the above-mentioned comb models, the fractional derivative models with distributed order, the heterogeneous process models with time or space dependent diffusion coefficient, the structural derivative models, and CTRW models have been consequently proposed. A survey of these models of ultraslow diffusion in heterogeneous materials is given in Ref. [27]. Among the existing models, the comb models directly connect the comb structure, but have complicated memory kernels, which can be also considered a class of fractional derivative model with distributed order. It is noted that the derivative order is a continuous statistical distribution with extra parameters and is determined empirically. The main issue is to simplify and improve the comb model for the extension of its applications in modeling ultraslow diffusion. Thus, one motivation of this study is to develop new comb models by selecting simpler memory kernels with clear physical meaning for modeling ultraslow diffusion in both the backbone and side branches.

In this study, to overcome the encountered problems, the comb model with new memory kernels is constructed based on the structural derivative used in the structural derivative models [28]. The structural derivative was proposed by Chen *et al.* [28] for modeling ultraslow diffusion using the logarithmic and inverse Mittag-Leffler (ML) functions as the memory kernel. The logarithmic function is a special case of the inverse ML function $E_\beta^{-1}(t)$ when $\beta = 1$. The inverse ML function is the inverse function of the famous ML function $E_\beta(t)$, which is defined by $E_\beta(t) = \sum_{n=0}^{\infty} \frac{t^n}{\Gamma(\beta n + 1)}$ [29]. In the structural derivative, the structural function plays a key role as a kernel transform of underlying time-space fabric of the complicated media [28], which includes local and nonlocal structural derivatives. The nonlocal structural derivative [30] includes the standard fractional derivative, and the recent proposed definitions of fractional derivatives with different kernel functions [31–33]. The structural derivative also has potential ability to model complex phenomena in diverse fields, such as superfast diffusion [34], control [35], creep [36], and anomalous diffusion [37].

The strategy to derive the structural derivative comb model in this study is adapted from that in [22] based on the classical 2D comb model, but to employ different memory kernels,

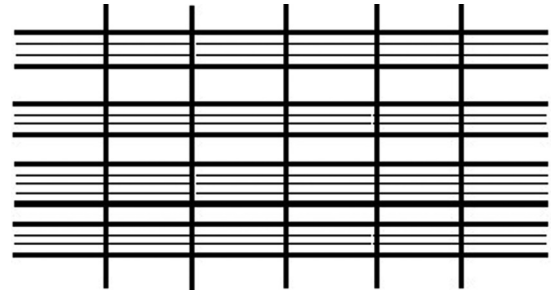


FIG. 2. Schematic diagram of fractal fracture of backbones.

such as the logarithmic function and the inverse ML function and their variants. In this study, the memory kernels are selected based on the patterns of ultraslow diffusion both in backbones and side branches. It has been mentioned that the logarithmic and inverse ML functions can be described by the MSD of ultraslow diffusion, and are feasible in construction of the nonlocal structural derivative ultraslow diffusion model as the structural function. The second motivation is to consider the reactive effect of the diffusive particles; in this study the first order catalytic reaction scheme $A + B \rightarrow 2A$ of the tracer in the backbone of the comblike structure is considered to construct the comb model, in which A is the catalyst. Another issue that should be pointed out is that for the comblike structures with spatial fractal geometry, non-Gaussian diffusions can be described by generalized comblike models [11,13,20,38]. Thus, in this study ultraslow diffusion in the fractal comb structure is also investigated as the third motivation by considering the spatial fractal geometry of the backbone volume $|x|^v$, where $0 < v < 1$ is the fractal dimension. Figure 2 gives a schematic diagram of the fractal fracture of the backbones.

The rest of this paper is organized as follows. Section II provides the comb model for ultraslow diffusion of reactive tracer, in which the first order catalytic reaction scheme is considered. In Sec. III, based on the model proposed in Sec. II, ultraslow diffusion process on a comb with fractal backbones is investigated. Finally, some concluding remarks are given in Sec. IV.

II. COMB MODEL FOR ULTRASLOW DIFFUSION OF TRACERS

In the present work, the first order catalytic reaction scheme $A + B \rightarrow 2A$ is considered [21]. The tracer is explored in the framework of a linear reactive transport equation using the comb model with the reaction kinetic term $Cu(x, y, t)$ [21]. Based on the two-dimensional comb model considered in Ref. [22], a general model for ultraslow diffusion is proposed with new kernel functions

$$\begin{aligned} & \int_0^t d\tau \gamma(t - \tau) \frac{\partial u(x, y, \tau)}{\partial \tau} \\ &= D_x \delta(y) \int_0^t d\tau \eta(t - \tau) \left[\frac{\partial^2 u(x, y, \tau)}{\partial x^2} + Cu(x, y, \tau) \right] \\ &+ D_y \frac{\partial^2 u(x, y, t)}{\partial y^2}. \end{aligned} \quad (1)$$

For Eq. (1), the initial condition is $u(x, y, 0) = \delta(x)\delta(y)$, and the boundary conditions for $u(x, y, \tau)$ and $\frac{\partial}{\partial q}u(x, y, t)$ are set to zero at infinity, where $q = \{x, y\}$. In Eq. (1), $\gamma(t)$ and $\eta(t)$ are memory kernel functions, which can be logarithmic or inverse ML functions. The reactive effect $Cu(x, y, \tau)$ is considered in the backbone of the comblike structure. For $C = 0$, the reaction term is equal to zero, and Eq. (1) can depict the ultraslow diffusion of the conservative tracer. It is also worth mentioning that the constant C can be greater ($C > 0$) or less than zero ($C < 0$). For the first case, we have an instantaneous creation process and for the second one, we have an instantaneous annihilation process. In this sense, it should be noted that the sign of C has a direct influence on the behavior of the MSDs. The delta function $\delta(y)$ in Eq. (1) means that the diffusion along the x direction is possible only in the backbone (at $y = 0$), while the side branches (fingers of the comb) play the role of traps in which the particle performs standard Brownian motion. Due to the trapping events in the fingers of the comb, which can be considered as waiting time for the particle, the motion along the backbone is slowed down in comparison to the corresponding one-dimensional motion. For the simplest case of diffusion process in the 2D comb ($\gamma(t) = \eta(t) = \delta(t)$ and $C = 0$) the motion along the backbone is subdiffusive with transport exponent $1/2$, i.e., $\langle x^2(t) \rangle \sim t^{1/2}$ [39].

The aim of Eq. (1) is to describe ultraslow diffusion in both x and y directions. Based on the definition of the nonlocal structural derivative [28], the kernel $\gamma(t)$ is the structural function, and Eq. (1) is a time structural derivative comb model.

By using Fourier-Laplace transform, solution of Eq. (1) in frequency domains reads

$$u(k_x, k_y, s) = \frac{s\gamma(s)\xi(s)}{[s\gamma(s) + D_y k_y^2] \left(s\xi(s) + \frac{1}{2} \frac{D_x}{\sqrt{D_y}} (k_x^2 - C) \right)}, \quad (2)$$

where $\xi(s) = \frac{1}{\eta(s)} \sqrt{\frac{\gamma(s)}{s}}$. The solution of Eq. (1) in the x direction is $u_1(x, t) = \int_{-\infty}^{\infty} dy u(x, y, t)$, and its corresponding Fourier-Laplace transform can be found by setting $k_y = 0$.

$$u_1(k_x, s) = \frac{\xi(s)}{s\xi(s) + \frac{1}{2} \frac{D_x}{\sqrt{D_y}} (k_x^2 - C)}. \quad (3)$$

Let us rewrite Eq. (3) as following

$$\begin{aligned} s\xi(s)u_1(k_x, s) - \xi(s) \\ = -\frac{1}{2} \frac{D_x}{\sqrt{D_y}} k_x^2 u_1(k_x, s) + \frac{1}{2} \frac{D_x}{\sqrt{D_y}} C u_1(k_x, s), \end{aligned} \quad (4)$$

from where by inverse Fourier-Laplace transformation we find the following generalized reaction-diffusion equation:

$$\begin{aligned} \int_0^t \xi(t-t') \frac{\partial}{\partial t'} u_1(x, t') dt' \\ = \frac{1}{2} \frac{D_x}{\sqrt{D_y}} \frac{\partial^2}{\partial x^2} u_1(x, t) + \frac{1}{2} \frac{D_x}{\sqrt{D_y}} C u_1(x, t). \end{aligned} \quad (5)$$

The solution of Eq. (5) in the Laplace domain can be found by inverse Fourier transform of Eq. (3), from where we find

$$\begin{aligned} u_1(x, s) = \frac{\xi(s)}{2} \sqrt{\frac{2\sqrt{D_y}}{D_x}} \left[s\xi(s) - C \frac{D_x}{2\sqrt{D_y}} \right]^{-1/2} \\ \times \exp \left[-\sqrt{\frac{2\sqrt{D_y}}{D_x}} s\xi(s) - C|x| \right]. \end{aligned} \quad (6)$$

Here we note that the solution is not normalized since

$$\langle x^0(t) \rangle = L^{-1} [u_1(k_x, s)]|_{k_x=0} = L^{-1} \left[\frac{\xi(s)}{s\xi(s) - \frac{D_x}{2\sqrt{D_y}} C} \right] \quad (7)$$

is different than 1. Only for $C = 0$, the solution is normalized and represents a probability density function (PDF). The second moment along the x direction yields

$$\begin{aligned} \langle x^2(t) \rangle = L^{-1} \left[-\frac{\partial^2}{\partial k_x^2} u_1(k_x, s) \right] \Big|_{k_x=0} \\ = \frac{D_x}{\sqrt{D_y}} L^{-1} \left\{ \xi(s) \left[s\xi(s) - \frac{1}{2} \frac{D_x}{\sqrt{D_y}} C \right]^{-2} \right\}, \end{aligned} \quad (8)$$

where $\eta(s)$ and $\gamma(s)$ are the Laplace pairs $\eta(t)$ and $\gamma(t)$, respectively.

The solution in the y direction can be obtained using a similar strategy, i.e., $u_2(y, t) = \int_{-\infty}^{\infty} dx u(x, y, t)$, and its Fourier-Laplace transform is expressed by

$$u_2(k_y, s) = \frac{s\gamma(s)\xi(s)}{[s\gamma(s) + D_y k_y^2] \left[s\xi(s) - \frac{1}{2} \frac{D_x}{\sqrt{D_y}} C \right]}. \quad (9)$$

We rewrite Eq. (9) in the following form,

$$\begin{aligned} \gamma(s)\xi(s)[su_2(k_y, s) - 1] \\ = -D_y k_y^2 \left[\xi(s) - \frac{1}{2} \frac{D_x}{\sqrt{D_y}} C s^{-1} \right] u_2(k_y, s) \\ + \frac{1}{2} \frac{D_x}{\sqrt{D_y}} C \gamma(s) u_2(k_y, s), \end{aligned} \quad (10)$$

and thus, by inverse Fourier-Laplace transforms we find the corresponding generalized equation,

$$\begin{aligned} \int_0^t \zeta(t-t') \frac{\partial}{\partial t'} u_2(y, t') dt' \\ = D_y \int_0^t \xi(t-t') \frac{\partial^2}{\partial y^2} u_2(y, t') dt' \\ - \frac{1}{2} D_x \sqrt{D_y} C \frac{\partial^2}{\partial y^2} \int_0^t u_2(y, t') dt', \\ + \frac{1}{2} \frac{D_x}{\sqrt{D_y}} C \int_0^t \gamma(t-t') u_2(y, t') dt', \end{aligned} \quad (11)$$

where $\zeta(t) = L^{-1}[\gamma(s)\xi(s)]$. The second moment along the y direction has the form

$$\begin{aligned} \langle y^2(t) \rangle &= L^{-1} \left[-\frac{\partial^2}{\partial k_y^2} u_2(k_y, s) \right] \Big|_{k_y=0} \\ &= 2D_y L^{-1} \left\{ \xi(s) \left[s^2 \gamma(s) \xi(s) - \frac{1}{2} s \gamma(s) \frac{D_x}{\sqrt{D_y}} C \right]^{-1} \right\}, \end{aligned} \quad (12)$$

and we also have

$$\langle y^0(t) \rangle = L^{-1} [u_2(k_y, s)] \Big|_{k_y=0} = L^{-1} \left[\frac{\xi(s)}{s\xi(s) - \frac{D_x}{2\sqrt{D_y}} C} \right]. \quad (13)$$

The solutions to the x and y directions $u_1(x, t)$ and $u_2(y, t)$, respectively, quantify the concentrations of the tracer, which can be directly derived by using the inverse Laplace and Fourier transforms.

To interpret the comb model in Eq. (1) in the framework of CTRW theory, the corresponding relationship between the kernel functions in the comb model and the densities for jump lengths and waiting time of the diffusive particles in the CTRW model are derived with $C = 0$ and dimensionless parameters $D_x = D_y = 1$. The diffusion process in the x direction can be easily simulated in which the density of jump lengths $\lambda(x)$ is a Gaussian distribution $N(0, 1)$ and the waiting time density has the Laplace transform $\phi_x(s) = \frac{1}{1+s\xi(s)}$. The corresponding CTRW model in the y direction has the same density of jump lengths, but the Laplace transform of the waiting time density is $\phi_y(s) = \frac{1}{1+s\gamma(s)}$. It should be pointed out that to keep the non-negativity of the solution and the waiting time PDFs, the memory kernels should satisfy conditions such that $\xi(s)$, $\gamma(s)$ should be completely monotone functions, and $s\xi(s)$, $s\gamma(s)$ should be Bernstein functions [22]. The corresponding PDFs can be found from (see, for example, [40])

$$\begin{aligned} u_{1,2}(x, t) &= \Phi_{x,y}(t) u_{1,2}(x, 0) \\ &+ \int_{-\infty}^{\infty} \int_0^t u_{1,2}(x', t') \psi_{x,y}(x - x', t - t') dt' dx', \end{aligned} \quad (14)$$

where $\psi_{x,y}(x, t) = \phi_{x,y}(t)\lambda(x)$ is the jump probability density of an uncoupled CTRW, and $\Phi_{x,y}(x, t) = 1 - \int_0^t \phi_{x,y}(t') dt'$ is the survival probability density that the walker does not take a step in time interval t . In the Fourier-Laplace domain these equations read as Eqs. (3) and (9) for $C = 0$.

Furthermore, the generalized reaction-diffusion equation (5) can be interpreted within the CTRW theory as well. Following the approach given in Ref. (40), the PDF of finding a particle at time t at position x in the backbone in case of CTRW with waiting time density $\phi_x(s) = \frac{1}{1+s\xi(s)} \approx 1 - s\xi(s)$ and Gaussian jump length density, in the presence of

instantaneous creation process, reads

$$\begin{aligned} u_1(x, t) &= r \Phi_x(t) u_1(x, 0) \\ &+ r \int_{-\infty}^{\infty} \int_0^t u_1(x', t') \phi_x(t - t') \lambda(x - x') dt' dx'. \end{aligned} \quad (15)$$

Here r gives the constant proportion of walkers added (or removed) instantaneously to the density of walkers that arrived at position x at time t , while $\Phi_x(s) = [1 - \phi_x(s)]/s \approx \xi(s)$. By Fourier-Laplace transform of this equation we arrive at Eq. (3) for $u_1(k_x, s)$, where constant C is related to the parameter r .

Here we note that one may also consider the 2D generalized reaction-diffusion equation, without constraints at $y = 0$, which means no Dirac delta function $\delta(y)$ in Eq. (1). In such a case for the marginal PDF along the backbone we find

$$\begin{aligned} &\int_0^t d\tau \gamma(t - \tau) \frac{\partial u_1(x, \tau)}{\partial \tau} \\ &= D_x \int_0^t d\tau \eta(t - \tau) \left[\frac{\partial^2 u_1(x, \tau)}{\partial x^2} + C u_1(x, \tau) \right], \end{aligned} \quad (16)$$

which is different than the corresponding equation for the marginal PDF in case of a comb structure; see Eq. (5). The second moment in this case becomes

$$\langle x^2(t) \rangle = 2D_x L^{-1} \{ \zeta(s) [s\zeta(s) - CD_x]^{-2} \}, \quad (17)$$

where $\zeta(s) = \gamma(s)/\eta(s)$.

For the simplest case with $\gamma(t) = \eta(t) = \delta(t)$, for the second moment we find $\langle x^2(t) \rangle = 2D_x L^{-1} [(s - CD_x)^{-2}] = 2D_x t e^{CD_x t}$ for $C > 0$, and $\langle x^2(t) \rangle = 2D_x t e^{-C^* D_x t}$ for $C = -C^* < 0$ ($C^* > 0$). For $C = 0$, the second moment becomes linear in time (normal diffusion), as it should be for a free diffusion process.

A. Cases with $\eta(t) = \delta(t)$

In this case, $\delta(t)$ is the Dirac function; the Laplace transform of the memory kernel is $\eta(s) = 1$.

Let us first consider the simplest case with $\gamma(t) = \delta(t)$, i.e., $\gamma(s) = 1$. This is a standard reaction-diffusion equation on a comb, where the reaction is along the backbone. Therefore, we have

$$\langle x^0(t) \rangle = L^{-1} \left[\frac{s^{-1/2}}{s^{1/2} - \frac{D_x}{2\sqrt{D_y}} C} \right] = E_{1/2} \left(\frac{D_x}{2\sqrt{D_y}} C t^{1/2} \right), \quad (18)$$

where $E_\alpha(z)$ is the one parameter Mittag-Leffler function, as defined before. From the asymptotic behavior of the one parameter ML function [41] $E_\alpha(z) \approx \frac{1}{\alpha} e^{z^{1/\alpha}}$, $z \rightarrow \infty$, for $C > 0$ in the long time limit we find $\langle x^0(t) \rangle \approx e^{\left(\frac{D_x}{2\sqrt{D_y}} C\right)^2 t}$, while for $C = -C^* < 0$ ($C^* > 0$), we have $\langle x^0(t) \rangle \approx \frac{2\sqrt{D_y}}{C^* D_x} t^{-1/2}$ since $E_\alpha(-\omega t^\alpha) \approx \frac{t^{-\alpha}}{\omega \Gamma(1-\alpha)}$, $t \rightarrow \infty$, $\omega > 0$.

The second moment along the backbone becomes

$$\begin{aligned} \langle x^2(t) \rangle &= \frac{D_x}{\sqrt{D_y}} L^{-1} \left[\frac{s^{-1/2}}{\left(s^{1/2} - \frac{D_x}{2\sqrt{D_y}} C \right)^2} \right] \\ &= \frac{D_x}{\sqrt{D_y}} t^{1/2} E_{1/2,3/2}^2 \left(\frac{D_x}{2\sqrt{D_y}} C t^{1/2} \right), \end{aligned} \quad (19)$$

where $E_{\alpha,\beta}^\gamma(z) = \sum_{n=0}^{\infty} \frac{(\gamma)_n}{\Gamma(\alpha n + \beta)} \frac{z^n}{n!}$ is the three parameter ML function, and $(\gamma)_n = \Gamma(\gamma + n)/\Gamma(\gamma)$ is the Pochhammer symbol. The short time limit yields $\langle x^2(t) \rangle \simeq \frac{D_x}{\sqrt{D_y}} \frac{t^{1/2}}{\Gamma(3/2)}$.

For $C > 0$, the second moment in the long time limit behaves as $\langle x^2(t) \rangle \simeq t e^{\left(\frac{D_x}{2\sqrt{D_y}} C\right)^2 t}$ since $E_{\alpha,\beta}^\gamma(z) \simeq \frac{1}{\alpha^\gamma} z^{(\gamma-\beta)/\alpha} e^{z^{1/\alpha}}$, $z \rightarrow \infty$ [41]. For $C = -C^* < 0$ ($C^* > 0$), we find $\langle x^2(t) \rangle \simeq \frac{4\sqrt{D_y}}{C^{*2} D_x} \frac{t^{-1/2}}{\Gamma(1/2)}$ since $E_{\alpha,\beta}^\gamma(-\omega t^\alpha) \simeq \frac{t^{-\alpha\gamma}}{\omega^\gamma \Gamma(\beta - \alpha\gamma)}$, $t \rightarrow \infty$, $\omega > 0$ [41]. For $C = 0$, we have $\langle x^0(t) \rangle = E_{1/2}(0) = 1$, and $\langle x^2(t) \rangle = \frac{D_x}{\sqrt{D_y}} t^{1/2} E_{1/2,3/2}^2(0) = \frac{D_x}{\sqrt{D_y}} \frac{t^{1/2}}{\Gamma(3/2)}$, as it should be for the diffusion in a 2D comb structure. Therefore, in the short time limit the reaction term does not change the dynamics in the comb structure. The second moment along the fingers becomes

$$\begin{aligned} \langle y^2(t) \rangle &= 2D_y L^{-1} \left[\frac{s^{-3/2}}{s^{1/2} - \frac{D_x}{2\sqrt{D_y}} C} \right] \\ &= 2D_y t E_{1/2,2} \left(\frac{D_x}{2\sqrt{D_y}} C t^{1/2} \right), \end{aligned} \quad (20)$$

where $E_{\alpha,\beta}(z) = E_{\alpha,\beta}^1(z)$ is the two parameter ML function. For short times it behaves as $\langle y^2(t) \rangle \simeq 2D_y t$ and for long times as $\langle y^2(t) \rangle \simeq e^{\left(\frac{D_x}{2\sqrt{D_y}} C\right)^2 t}$ for $C > 0$, and as $\langle y^2(t) \rangle \simeq t^{1/2}$ for $C < 0$. Similarly to the previous result for the x direction, the reaction term does not change the dynamics in the y direction for short times. For $C = 0$, we have $\langle y^2(t) \rangle = 2D_y t E_{1/2,2}(0) = 2D_y t$.

The kernel function $\gamma(t)$ is selected as

$$\gamma(t) = \ln^{-\alpha}(t), \quad (21)$$

where $\alpha > 0$. In this case, $\gamma(t)$ is a slowly varying function at infinity. By using the Tauberian theorem, the Laplace transform of Eq. (21) is

$$\gamma(s) \simeq \frac{1}{s \ln^\alpha(1/s)}. \quad (22)$$

The asymptotic behavior of the second moment along the x direction is derived as

$$\langle x^2(t) \rangle \simeq \frac{D_x}{\sqrt{D_y}} L^{-1} \left\{ \frac{1}{s} \ln^{-\frac{\alpha}{2}} \left(\frac{1}{s} \right) \left[\ln^{-\frac{\alpha}{2}} \left(\frac{1}{s} \right) - \frac{D_x}{2\sqrt{D_y}} C \right]^{-2} \right\}, \quad (23)$$

and along the y direction as

$$\langle y^2(t) \rangle \simeq 2D_y L^{-1} \left\{ \frac{1}{s} \ln^{\frac{\alpha}{2}} \left(\frac{1}{s} \right) \left[\ln^{-\frac{\alpha}{2}} \left(\frac{1}{s} \right) - \frac{D_x}{2\sqrt{D_y}} C \right]^{-1} \right\}. \quad (24)$$

The cases for the conservative tracer when $C = 0$, for the MSD along the x and y directions, by using the Tauberian theorem [22], give

$$\langle x^2(t) \rangle \simeq \frac{D_x}{\sqrt{D_y}} L^{-1} \left[\frac{1}{s} \ln^{\frac{\alpha}{2}} \left(\frac{1}{s} \right) \right] \simeq \frac{D_x}{\sqrt{D_y}} \ln^{\frac{\alpha}{2}}(t), \quad (25)$$

$$\langle y^2(t) \rangle \simeq 2D_y L^{-1} \left[\frac{1}{s} \ln^\alpha \left(\frac{1}{s} \right) \right] \simeq 2D_y \ln^\alpha(t), \quad (26)$$

respectively, which were also obtained by considering power-law distributed order memory kernel [22]. Thus, in this case the two-dimensional comb model can depict the ultraslow diffusion along both the x and y directions. When $\alpha = 4$, the dynamics in the y direction is the classical Sinai diffusion [27]. The corresponding concentrations then behave as

$$u_1(x, t) \simeq \frac{1}{2} \left(\frac{2\sqrt{D_y}}{D_x} \right)^{\frac{1}{2}} \frac{1}{\ln^{\frac{\alpha}{4}}(t)} \exp \left[- \left(\frac{2\sqrt{D_y}}{D_x} \right)^{\frac{1}{2}} \frac{|x|}{\ln^{\alpha/4}(t)} \right], \quad (27)$$

and

$$u_2(y, t) \simeq \frac{1}{2\sqrt{D_y}} \frac{1}{\ln^{\frac{\alpha}{2}}(t)} \exp \left[- \frac{|y|}{\sqrt{D_y} \ln^{\alpha/2}(t)} \right]. \quad (28)$$

To interpret the ultraslow diffusion from the perspective of CTRW theory, the waiting time density to the x direction is derived as

$$\begin{aligned} \phi_x(s) &\simeq 1 - s \xi(s) \simeq 1 - s \left[\frac{s^{-1}}{\ln^{\frac{\alpha}{2}} \left(\frac{1}{s} \right)} \right], \quad s \rightarrow 0 \\ &\rightarrow \phi_x(t) \simeq - \frac{d}{dt} \xi(t) \simeq - \frac{d}{dt} \left[\frac{1}{\ln^{\frac{\alpha}{2}}(t)} \right] \\ &= \frac{\alpha/2}{t [\ln(t)]^{\alpha/2+1}}, \quad t \rightarrow \infty, \end{aligned} \quad (29)$$

and to the y direction as

$$\begin{aligned} \phi_y(s) &\simeq 1 - s \gamma(s) \simeq 1 - s \left[\frac{s^{-1}}{\ln^\alpha \left(\frac{1}{s} \right)} \right], \quad s \rightarrow 0 \\ &\rightarrow \phi_y(t) \simeq - \frac{d}{dt} \gamma(t) \simeq - \frac{d}{dt} \left[\frac{1}{\ln^\alpha(t)} \right] \\ &= \frac{\alpha}{t [\ln(t)]^{\alpha+1}}, \quad t \rightarrow \infty. \end{aligned} \quad (30)$$

Using the same strategy, a general memory kernel function can be selected to derive the MSDs and solutions of the corresponding ultraslow diffusion processes. When the inverse ML

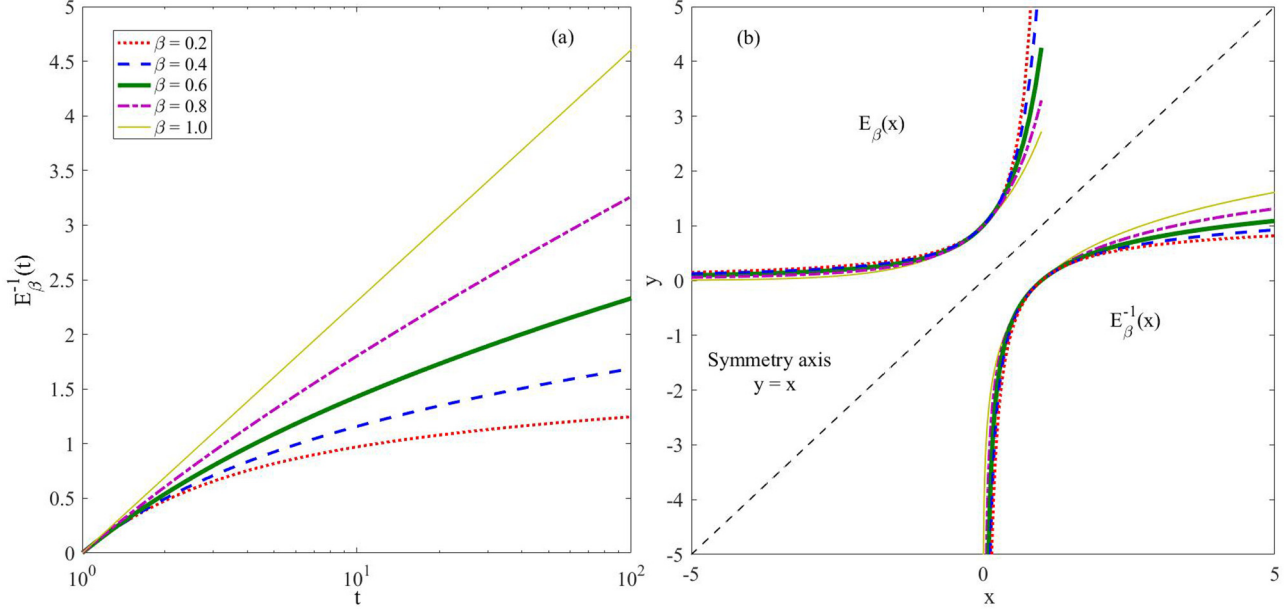


FIG. 3. Plots of (a) the inverse Mittag-Leffler function versus time t for $\beta = 0.2, 0.4, 0.6, 0.8, 1.0$ from bottom to top, and (b) the Mittag-Leffler function and its inverse case versus position x for $\beta = 0.2, 0.4, 0.6, 0.8, 1.0$. The legend of (b) is the same as in (a).

function $[E_\beta^{-1}(t/t_0)]^{-\alpha}$ is selected, which is a slowly varying function at infinity, it generalizes the logarithmic memory function. Here t_0 is a constant used to keep the dimension consistent. It should be pointed out that in the following cases for the inverse ML cases, we select the dimensionless time t ,

$$\gamma(t) = [E_\beta^{-1}(t)]^{-\alpha}, \tag{31}$$

where $\alpha > 0$ and $0 < \beta \leq 1$. When $\beta = 1$, $E_1^{-1}(t)$ is the logarithmic function $\ln(t)$. The inverse ML function does not have a closed form. However, it can be numerically calculated by using the famed ML function. Figure 3 shows the patterns of inverse ML function $E_\beta^{-1}(t)$ and its connections with the ML function $E_\beta(t)$ for five different values of parameter β . From Fig. 3(a), it is observed that the smaller the value of β is, the slower is the increase rate obtained. In the semilogarithmic axial of t , the curves are almost a straight line for the large values of time t . Figure 3(b) shows five pairs of ML and inverse ML functions, which are symmetric by the straight line $y = x$. The legend of Fig. 3(b) is the same as that of Fig. 3(a).

The Laplace transform of Eq. (31) is

$$\gamma(s) \simeq \frac{1}{s[E_\beta^{-1}(\frac{1}{s})]^\alpha}. \tag{32}$$

For $C = 0$, by using the Tauberian theorem, for the MSDs we find

$$\langle x^2(t) \rangle \simeq \frac{D_x}{\sqrt{D_y}} [E_\beta^{-1}(t)]^{\alpha/2}, \tag{33}$$

$$\langle y^2(t) \rangle \simeq 2D_y [E_\beta^{-1}(t)]^\alpha, \tag{34}$$

while the corresponding PDFs behave as

$$u_1(x, t) \simeq \frac{1}{2} \left(\frac{2\sqrt{D_y}}{D_x} \right) \frac{1}{[E_\beta^{-1}(t)]^{\frac{\alpha}{4}}} \times \exp \left[- \left(\frac{2\sqrt{D_y}}{D_x} \right)^{\frac{1}{2}} \frac{|x|}{[E_\beta^{-1}(t)]^{\frac{\alpha}{4}}} \right], \tag{35}$$

$$u_2(y, t) \simeq \frac{1}{2D_y} \frac{1}{[E_\beta^{-1}(t)]^{\frac{\alpha}{2}}} \exp \left(- \frac{|y|}{\sqrt{D_y} [E_\beta^{-1}(t)]^{\frac{\alpha}{2}}} \right). \tag{36}$$

Equations (33) and (34) can describe generalized ultraslow diffusion, which is respectively degenerate to Eqs. (25) and (26) for $\beta = 1$.

The waiting time density for the conservative tracer to the x direction is

$$\phi_x(s) \simeq 1 - s\xi(s) \simeq 1 - s \left\{ \frac{s^{-1}}{[E_\beta^{-1}(\frac{1}{s})]^{\alpha/2}} \right\},$$

$$\rightarrow \phi_x(t) \simeq -\frac{d}{dt} \xi(t) \simeq -\frac{d}{dt} \left\{ \frac{1}{[E_\beta^{-1}(t)]^{\alpha/2}} \right\}. \tag{37}$$

and to the y direction is

$$\phi_y(s) \simeq 1 - s\gamma(s) \simeq 1 - s \left\{ \frac{s^{-1}}{[E_\beta^{-1}(\frac{1}{s})]^\alpha} \right\},$$

$$\rightarrow \phi_y(t) \simeq -\frac{d}{dt} \gamma(t) \simeq -\frac{d}{dt} \left\{ \frac{1}{[E_\beta^{-1}(t)]^\alpha} \right\}. \tag{38}$$

In the above two cases, the logarithmic and inverse ML functions are used as the memory kernel in the comb model, which can be considered as a structural function of the time structural derivative. It should be pointed out that the fractional derivative comb model with a power-law memory kernel can describe subdiffusion in both backbone and side branches [22]. But the comb model can describe ultraslow diffusion when the kernel function is a distributed function with an integral form, i.e., the distributed order fractional derivative comb model, in which the distributed order of the fractional derivative modifies the constant order in the fractional derivative by integrating all possible orders over a certain range [22]. When the distributed order is a uniform distribution or a more general power-law distribution, it can describe ultraslow diffusion, and its corresponding MSDs are almost equivalent with those of the comb model derived in this study. Compared with the existing fractional derivative comb models, the structural derivative comb model with a logarithmic memory kernel is with simpler mathematical form or fewer parameters, and its memory kernel has a clear correlation with the MSDs and PDFs of the displacement and waiting time density.

B. Case with $\eta(t) = \frac{t^{-\mu}}{\Gamma(1-\mu)}$

The Laplace transform of $\eta(t)$ is

$$\eta(s) = s^{\mu-1}. \quad (39)$$

Here we use $1/2 < \mu < 1$ [22].

First we consider the simple case of $\gamma(t) = \delta(t)$. Therefore, we find

$$\begin{aligned} \langle x^0(t) \rangle &= L^{-1} \left[\frac{s^{-\mu+1/2}}{s^{-\mu+3/2} - \frac{D_x}{2\sqrt{D_y}} C} \right] \\ &= E_{3/2-\mu} \left(\frac{D_x}{2\sqrt{D_y}} C t^{3/2-\mu} \right), \end{aligned} \quad (40)$$

and

$$\begin{aligned} \langle x^2(t) \rangle &= \frac{D_x}{\sqrt{D_y}} L^{-1} \left[\frac{s^{-\mu+1/2}}{\left(s^{-\mu+3/2} - \frac{D_x}{2\sqrt{D_y}} C \right)^2} \right] \\ &= \frac{D_x}{\sqrt{D_y}} t^{3/2-\mu} E_{3/2-\mu, 5/2-\mu} \left(\frac{D_x}{2\sqrt{D_y}} C t^{3/2-\mu} \right), \end{aligned} \quad (41)$$

which in the long time limit behaves as $\langle x^2(t) \rangle \simeq t \exp\left[\left(\frac{D_x}{2\sqrt{D_y}} C\right)^{2/(3-2\mu)} t\right]$ for $C > 0$, and saturates for $C < 0$, i.e., $\langle x^2(t) \rangle \simeq \text{const.}$ For $C = 0$ we recover the result given in Ref. [22],

$$\langle x^2(t) \rangle = \frac{D_x}{\sqrt{D_y}} t^{3/2-\mu} E_{3/2-\mu, 5/2-\mu}(0) = \frac{D_x}{\sqrt{D_y}} \frac{t^{3/2-\mu}}{\Gamma(5/2-\mu)}. \quad (42)$$

Moreover, the second moment along the fingers reads

$$\begin{aligned} \langle y^2(t) \rangle &= 2D_y L^{-1} \left[\frac{s^{-\mu-1/2}}{s^{-\mu+3/2} - \frac{D_x}{2\sqrt{D_y}} C} \right] \\ &= 2D_y t E_{\frac{3}{2}-\mu, 2} \left(\frac{D_x}{2\sqrt{D_y}} C t^{3/2-\mu} \right), \end{aligned} \quad (43)$$

which in the long time limit grows exponentially in time, $\langle y^2(t) \rangle \simeq \exp\left[\left(\frac{D_x}{2\sqrt{D_y}} C\right)^{2/(3-2\mu)} t\right]$, for $C > 0$, and as a power law, $\langle y^2(t) \rangle \simeq t^{\mu-1/2}$, for $C < 0$. For $C = 0$, one finds that $\langle y^2(t) \rangle = 2D_y t E_{\frac{3}{2}-\mu, 2}(0) = 2D_y t$, as it should be.

When the kernel function $\gamma(t)$ is $\gamma(t) = \ln^{-\alpha}(t)$, the MSDs along the x and y directions become

$$\langle x^2(t) \rangle \simeq \frac{D_x}{\sqrt{D_y}} L^{-1} \left[\frac{s^{-\mu} \ln^{-\alpha/2}\left(\frac{1}{s}\right)}{\left(s^{1-\mu} \ln^{-\frac{\alpha}{2}}\left(\frac{1}{s}\right) - \frac{D_x}{2\sqrt{D_y}} C \right)^2} \right], \quad (44)$$

and

$$\langle y^2(t) \rangle \simeq 2D_y L^{-1} \left[\frac{s^{-\mu} \ln^{-\alpha/2}\left(\frac{1}{s}\right)}{s^{1-\mu} \ln^{-\frac{\alpha}{2}}\left(\frac{1}{s}\right) - \frac{D_x}{2\sqrt{D_y}} C} \right]. \quad (45)$$

For the conservative tracer, $C = 0$, Eq. (44) degenerates to

$$\langle x^2(t) \rangle \simeq \frac{D_x}{\sqrt{D_y}} t^{1-\mu} \ln^{\alpha/2}(t). \quad (46)$$

We see that the diffusion is faster than the case for $\eta(t) = \delta(t)$ due to the power-law term, which appears as a result of the compensation memory kernel $\eta(t) = t^{-\mu}/\Gamma(1-\mu)$. Similarly, for $C = 0$, the MSD along the fingers becomes

$$\langle y^2(t) \rangle \simeq 2D_y \ln^{\alpha}(t). \quad (47)$$

While the corresponding PDFs behaves as

$$\begin{aligned} u_1(x, t) &\sim \frac{\sqrt{D_y^{1/2}}}{D_x^{1/2}} \left[t^{\mu-1} \ln^{-\frac{\alpha}{2}}(t) \right]^{1/2} \\ &\times \exp \left(- \left[\frac{2\sqrt{D_y}}{D_x} t^{\mu-1} \ln^{-\frac{\alpha}{2}}(t) \right]^{1/2} |x| \right), \end{aligned} \quad (48)$$

and

$$u_2(y, t) \sim \left[\frac{1}{2\sqrt{D_y} \ln^{\alpha}(t)} \right] \exp \left(- \frac{|y|}{\sqrt{D_y}} \right). \quad (49)$$

To check the connections and differences for the conservative and reactive tracers, Fig. 4(a) illustrates the MSDs for the reactive [Eqs. (23) and (24)] and conservative tracers [Eqs. (25) and (26)], with dimensionless parameters $D_x = D_y = 1$, $\alpha = 1$, $C = 0.1$. The inverse Laplace transforms in the equations are numerically calculated. It can be observed, from Fig. 4(a), that the diffusion process in the y direction is faster than that in the x direction based on the results of MSDs. Considering the reactive effects, the differences of the MSDs between the conservative and reactive tracers are clear. Compared with power-law and logarithmic functions the ultraslow diffusion process often occurs in the long-time scale

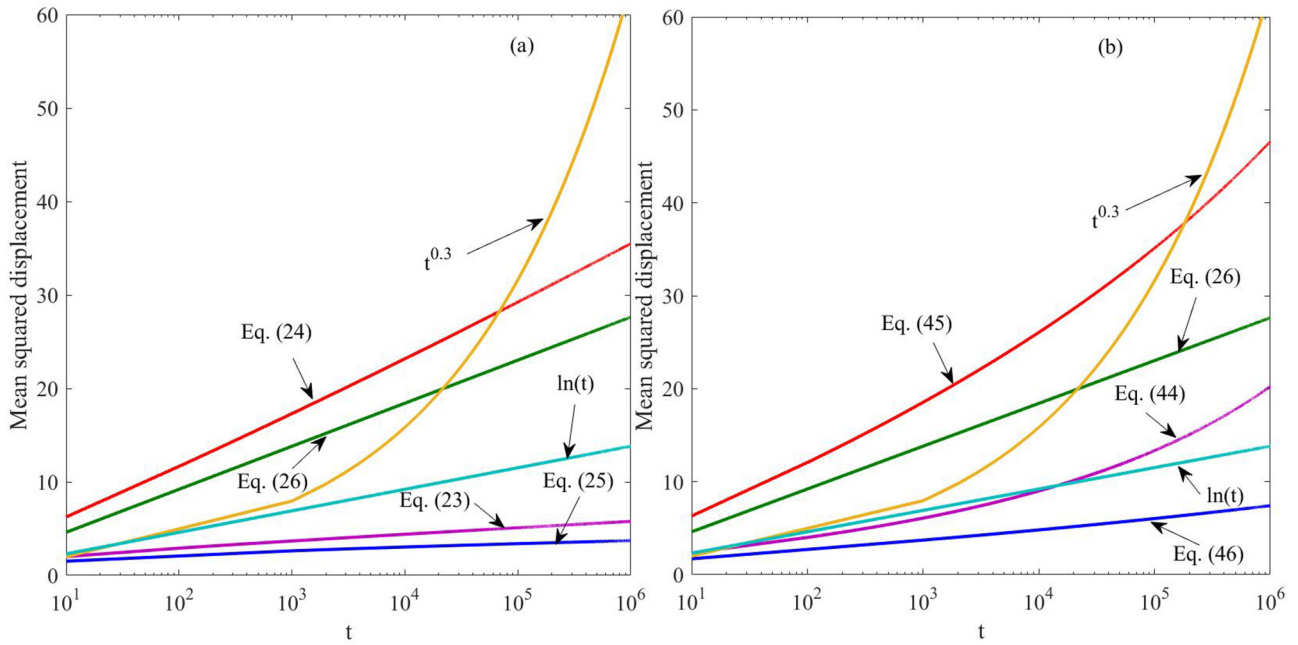


FIG. 4. Plots of (a) MSDs for the reactive [Eqs. (23) and (24)] and conservative tracers [Eqs. (25) and (26)], and (b) MSDs for the reactive [Eqs. (44) and (45)] and conservative tracers [Eqs. (46) and (26)] with dimensionless parameters $D_x = D_y = 1$, $\alpha = 1$, $\mu = 0.95$, $C = 0.1$.

limit, particularly in the backbone of the comblike structure. To check the influence of a different form for the memory kernel $\eta(t)$, Fig. 4(b) provides the MSDs for the reactive [Eqs. (44) and (45)] and conservative tracers [Eqs. (46) and (26)]. It is found that, from Fig. 4(b), the results of the MSDs have a similar pattern to those in Fig. 4(a) for small value $\mu = 0.95$.

To check the reactive effect considered in the backbone of the comblike structure, Fig. 5 gives the MSDs in Eqs. (23)

and (44) with dimensionless parameters $D_x = D_y = 1$, $\alpha = 1$, $\mu = 0.95$, and different values of C . It can be observed from Figs. 5(a) and 5(b) that with larger positive C , the MSD grows much faster than that of the conservative tracer with $C = 0$, and the underlying diffusion is a creation process. It is also noted that the MSDs in Fig. 5(a) with $C = 0.5$ and in Fig. 5(b) with $C = 0.3$ grow even faster than the power law for the subdiffusion process. For negative C in Figs. 5(a) and 5(b), the MSD grows even slower than the conservative case, and

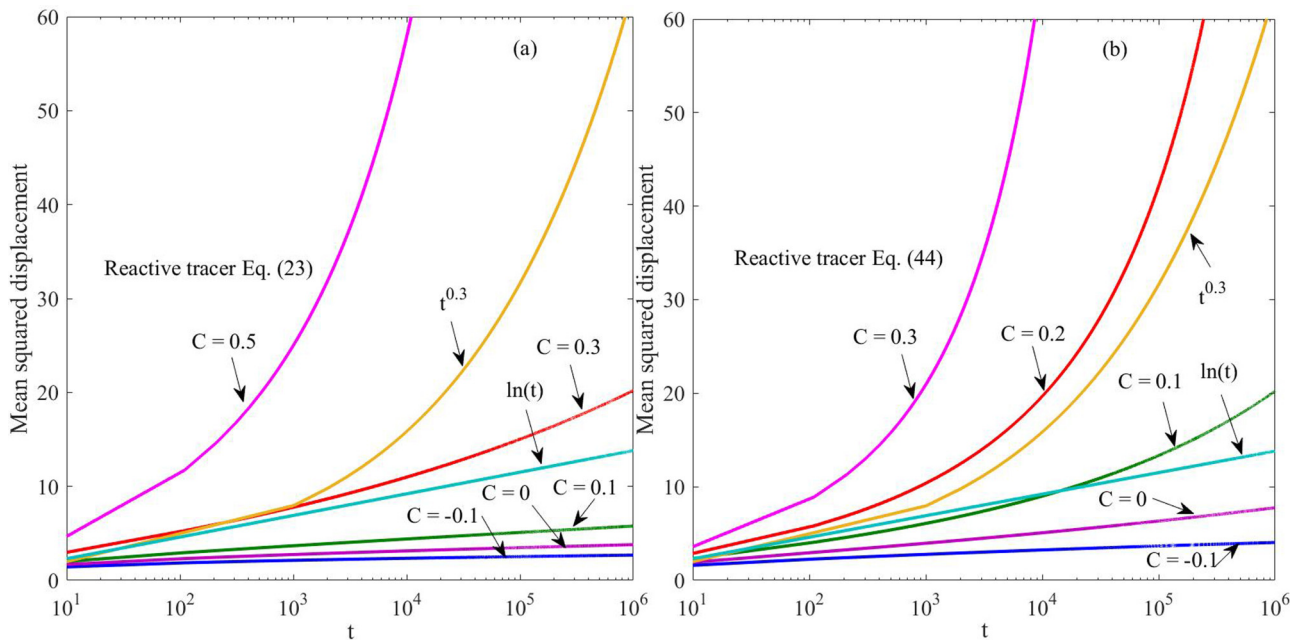


FIG. 5. Plots of (a) MSDs in Eq. (23), and (b) MSDs in Eq. (44) with dimensionless parameters $D_x = D_y = 1$, $\alpha = 1$, $\mu = 0.95$, and different values of C .

the diffusion is an instantaneous annihilation process. Thus, the sign of C has a direct influence on the behavior of the MSDs.

In comb models, the kernel $\gamma(t)$ is responsible for slowing down the motion along the backbone, while the kernel $\eta(t)$ may accelerate it, in comparison to the diffusion in the standard comb model where the MSD behaves as $t^{1/2}$ [39]. Thus, the kernel $\eta(t)$ is also called a *compensation kernel* [22]. The slowed motion caused by $\gamma(t)$ may be compensated by an appropriate kernel $\eta(t)$. This is evident if one compares the results for the second moments in the case of a Dirac delta memory kernel and a power-law memory kernel. However, both kernels should be such that the non-negativity of the corresponding solutions is preserved. Therefore, the structural derivative comb model is feasible to describe the ultraslow diffusions both in the backbones and side branches of the comblike structure.

III. ULTRASLOW DIFFUSION ON A FRACTAL COMB

Ultraslow diffusion may occur not only in a single backbone, but also if one considers many backbones, located at $y = l_j, j = 1, 2, \dots, N$, and $0 \leq l_1 < l_2 < \dots < l_N$. In this section we consider a fractal structure of backbones: $l_j \in S_v, S_v$ is the fractal structure, and $0 < v < 1$ is the fractal dimension. To describe diffusion on such fractal structure, Eq. (1) should be generalized as

$$\int_0^t d\tau \gamma(t - \tau) \frac{\partial u(x, y, \tau)}{\partial \tau} = D_x \sum_{j=1}^N \delta(y - l_j) \int_0^t d\tau \eta(t - \tau) \times \left[\frac{\partial^2 u(x, y, \tau)}{\partial x^2} + C u(x, y, \tau) \right] + D_y \frac{\partial^2 u(x, y, t)}{\partial y^2}. \tag{50}$$

where the initial condition is $u(x, y, 0) = \delta(x)\delta(y), l_j \in S_v$. The conditions of the boundaries for $u(x, y, \tau)$ and $\frac{\partial}{\partial q} u(x, y, t), q = \{x, y\}$ are zero at infinity; $x = \pm\infty, y = \pm\infty, \gamma(t)$, and $\eta(t)$ are kernel functions. The integral with respect to t is in fact an approximation in the limit of an infinite number of backbones. Here we note that for $v = 0$, Eq. (50) reduces to Eq. (1). The Laplace transform of Eq. (50) reads

$$s\gamma(s)u(x, y, s) - \gamma(s)u(x, y, t = 0) = D_x \sum_{j=1}^N \delta(y - l_j)\eta(s) \times \left[\frac{\partial^2 u(x, y, s)}{\partial x^2} + C u(x, y, s) \right] + D_y \frac{\partial^2 u(x, y, s)}{\partial y^2}. \tag{51}$$

Let us represent the solution $u(x, y, s)$ as [11,38]

$$u(x, y, s) = f(x, s) \exp \left[-\sqrt{\frac{s\gamma(s)}{D_y}} |y| \right], \tag{52}$$

and use $G(x, s) = \int_{-\infty}^{+\infty} u(x, y, s) dy$. Then we integrate Eq. (51) in respect to y ,

$$s\gamma(s)G(x, s) - \gamma(s)G(x, t = 0) = D_x \eta(s) \left\{ \frac{\partial^2}{\partial x^2} \left[\sum_{j=1}^N u(x, y = l_j, s) \right] + C \sum_{j=1}^N u(x, y = l_j, s) \right\}, \tag{53}$$

in which

$$\sum_{j=1}^N u(x, y = l_j, s) = \sum_{j=1}^N f(x, s) \exp \left[-\sqrt{\frac{s\gamma(s)}{D_y}} |l_j| \right] = \frac{f(x, s)}{\Gamma(v)} \int_0^\infty l^{v-1} \exp \left[-\sqrt{\frac{s\gamma(s)}{D_y}} l \right] dl = f(x, s) \left[\frac{D_y}{s\gamma(s)} \right]^{v/2} = \frac{1}{2D_y^{\frac{1-v}{2}}} [s\gamma(s)]^{\frac{1-v}{2}} G(x, s). \tag{54}$$

From Eq. (54), Eq. (53) can be rewritten as

$$sG(x, s) - G(x, t = 0) = \frac{D_x}{2D_y^{\frac{1-v}{2}}} \frac{s^{\frac{1-v}{2}} \eta(s)}{[\gamma(s)]^{\frac{1+v}{2}}} \left[\frac{\partial^2 G(x, s)}{\partial x^2} + C G(x, s) \right]. \tag{55}$$

The Fourier transform of Eq. (55) is

$$sG(k_x, s) - G(k_x, t = 0) = \frac{D_x}{2D_y^{\frac{1-v}{2}}} \frac{s^{\frac{1-v}{2}} \eta(s)}{[\gamma(s)]^{\frac{1+v}{2}}} \left[-k_x^2 G(k_x, s) + C G(k_x, s) \right], \tag{56}$$

and thus we obtain

$$G(k_x, s) = \frac{\rho(s)}{s\rho(s) + \frac{1}{2} \frac{D_x}{D_y^{\frac{1-v}{2}}} (k_x^2 - C)}, \tag{57}$$

where $\rho(s) = \frac{[\gamma(s)]^{\frac{1+v}{2}}}{s^{\frac{1-v}{2}} \eta(s)}$.

The second moment along the x direction yields the following general form:

$$\langle x^2(t) \rangle = L^{-1} \left[-\frac{\partial^2}{\partial k_x^2} u(k_x, s) \right] \Big|_{k_x=0} = \frac{D_x}{D_y^{\frac{1-v}{2}}} L^{-1} \left\{ \rho(s) \left[s\rho(s) - \frac{1}{2} \frac{D_x}{D_y^{\frac{1-v}{2}}} C \right]^{-2} \right\}. \tag{58}$$

By using similar memory kernels as in Sec. II, we derive the MSDs and the corresponding solutions. To interpret the comb model in Eq. (50) from the context of CTRW theory, the corresponding relationship between the kernel functions

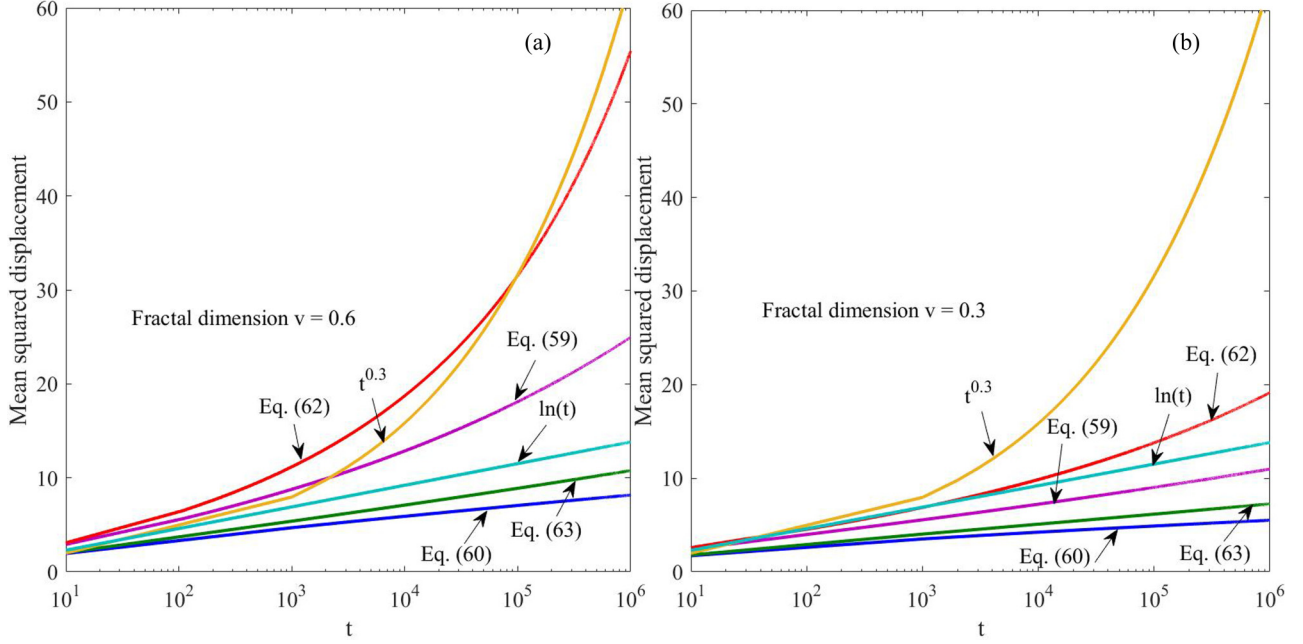


FIG. 6. Plots of MSDs to the fractal backbones for the reactive [Eqs. (59) and (60)] and conservative tracers [Eqs. (62) and (63)] with dimensionless parameters $D_x = D_y = 1$, $\alpha = 1$, $\mu = 0.98$, $C = 0.1$.

in the comb model, the fractal dimension of the backbones, and the densities for jump lengths and waiting time of the diffusive particles in the CTRW model are derived with $C = 0$ and dimensionless parameters $D_x = D_y = 1$. The diffusion processes can be simulated in which the density of jump lengths is the Gaussian distribution $N(0, 1)$ and the waiting time density to the x direction has the Laplace transform $\omega_x(s) = \frac{1}{1+s\rho(s)}$, and to the y direction is given as $\omega_y(s) = \frac{1}{1+s\gamma(s)}$.

A. Cases with $\eta(t) = \delta(t)$

The kernel function $\gamma(t)$ is selected as $\gamma(t) = \ln^{-\alpha}(t)$, $\alpha > 0$. The second moment along the x direction is

$$\langle x^2(t) \rangle \simeq \frac{D_x}{D_y^{\frac{1-v}{2}}} L^{-1} \left[\frac{\frac{1}{s} \ln^{-\frac{(1+v)\alpha}{2}}(1/s)}{(\ln^{-\frac{(1+v)\alpha}{2}}(1/s) - \frac{1}{2} \frac{D_x}{D_y^{\frac{1-v}{2}}} C)^2} \right]. \quad (59)$$

Moreover, for the conservative tracer ($C = 0$), the MSD along the x direction is given by

$$\langle x^2(t) \rangle \simeq \frac{D_x}{D_y^{\frac{1-v}{2}}} \ln^{\frac{(1+v)\alpha}{2}}(t). \quad (60)$$

In this case, the corresponding solution for the conservative tracer becomes

$$u_1(x, t) \sim \frac{\sqrt{D_y^{1/2-v/2}}}{\sqrt{2D_x \ln^{(1+v)\alpha/2}(t)}} \exp \left[-\frac{\sqrt{2D_y^{1/2-v/2}}|x|}{\sqrt{D_x \ln^{(1+v)\alpha/2}(t)}} \right]. \quad (61)$$

For the generalized kernel function $\gamma(t) = [E_\mu^{-1}(t)]^\alpha$, the second moment and solution can be obtained in a similar way.

B. Case with $\eta(t) = \frac{t^{-\mu}}{\Gamma(1-\mu)}$

For the kernel function $\gamma(t)$ is $\gamma(t) = \ln^{-\alpha}(t)$, and the MSDs along the x direction are

$$\langle x^2(t) \rangle \simeq \frac{D_x}{D_y^{\frac{1-v}{2}}} L^{-1} \left\{ \frac{s^{-\mu} \ln^{-\frac{(1+v)\alpha}{2}}(1/s)}{[s^{1-\mu} \ln^{-\frac{(1+v)\alpha}{2}}(1/s) - \frac{1}{2} \frac{D_x}{D_y^{\frac{1-v}{2}}} C]^2} \right\}. \quad (62)$$

For the conservative tracer, the MSD reads

$$\langle x^2(t) \rangle \simeq \frac{D_x}{D_y^{\frac{1-v}{2}}} t^{1-\mu} \ln^{\frac{(1+v)\alpha}{2}}(t), \quad (63)$$

and the PDF becomes

$$u_1(x, t) \sim \frac{\sqrt{D_y^{1/2-v/2}}}{\sqrt{2D_x t^{1-\mu} \ln^{(1+v)\alpha/2}(t)}} \times \exp \left[-\frac{\sqrt{2D_y^{1/2-v/2}}|x|}{\sqrt{D_x t^{1-\mu} \ln^{(1+v)\alpha/2}(t)}} \right]. \quad (64)$$

To check the influence of the fractal dimension of the backbones, Figs. 6(a) and 6(b) provide the MSDs for the reactive and conservative tracers when the fractal dimension is $v = 0.6$ and $v = 0.3$, respectively. The results show that smaller fractal dimension decelerates ultraslow diffusion. We can also observe from Fig. 6 that the reaction effect accelerates ultraslow diffusion which is consistent with the cases shown in Fig. 4. Thus, it is feasible that such comb model can describe the ultraslow diffusions in comblike structure with fractal backbones.

IV. SUMMARY

In this study ultraslow diffusion of tracers in comb-like structure is investigated by a two-dimensional reaction-diffusion equation with two memory kernels for a two-dimensional comb. The first order catalytic reaction scheme is considered in the frame of the comb model, which is solved by using the inverse Laplace-Fourier transform on the general expressions of the solutions in frequency domains. The logarithmic and inverse Mittag-Leffler functions are selected as the kernels, which are frequently used in the structural derivative models. The solutions and the corresponding mean squared displacements (MSDs) are derived for the different memory kernels. The solutions follow a double-sided exponential distribution. Compared with the conservative cases, the reactive effect does not change the patterns of MSDs and solutions, which accelerates the ultraslow diffusion both on the x and y directions. Based on the proposed comb model, ultraslow diffusion on a generalized fractal comb of the backbones is also considered. The derived MSDs and solutions depend on the fractal dimension of backbones. Thus, the comb model is useful to describe the ultraslow diffusions in both the backbones and side branches of the comb. In further study, the comb model should be tested with real applications, and the effects of the nonlinear reaction scheme will also be discussed. To place the comb models in a more general perspective, the recent work [42] on systematic analysis of the

projection-induced non-Markovian dynamics and anomalous diffusion should be discussed in the future study.

ACKNOWLEDGMENTS

The work described in this paper was supported by the National Natural Science Foundation of China (Grant No. 11702085), and the Fundamental Research Funds for the Central Universities (Grant No. 2019B16114). T.S. was supported by the Alexander von Humboldt Foundation.

APPENDIX: TAUBERIAN THEOREM FOR SLOWLY VARYING FUNCTIONS

In the Tauberian theorem [22], for the function $f(t)$, $t \geq 0$, when its Laplace transform has the following asymptotic form,

$$f(s) \simeq s^{-\theta} G\left(\frac{1}{s}\right), \quad s \rightarrow 0, \quad \theta \geq 0, \quad (\text{A1})$$

then the function $f(t)$ satisfies

$$f(t) = L^{-1}[r(s)] \simeq \frac{1}{\Gamma(\theta)} t^{\theta-1} G(t), \quad t \rightarrow \infty, \quad (\text{A2})$$

where $G(t)$ should be a slowly varying function at infinity, which satisfies $\lim_{t \rightarrow \infty} \frac{G(at)}{G(t)} = 1$, $a > 0$.

-
- [1] S. Yuste, E. Abad, and A. Baumgaertner, Anomalous diffusion and dynamics of fluorescence recovery after photobleaching in the random-comb model, *Phys. Rev. E* **94**, 012118 (2016).
 - [2] A. Polotsky, T. Birshstein, A. Mercurieva, F. Leermakers, and O. Borisov, Unfolding of a comb-like polymer in a poor solvent: translation of macromolecular architecture in the force-deformation spectra, *Soft Matter* **13**, 9147 (2017).
 - [3] X. Zhao, X. Li, K. Zhao, and Y. Tang, Preparation of a hydroxyapatite ceramic with comblike tubules structure and its permeability, *Key Eng. Mater.* **768**, 135 (2018).
 - [4] A. Sylvester, The nature and polygenetic origin of orbicular granodiorite in the Lower Castle Creek pluton, northern Sierra Nevada batholith, California, *Geosphere* **7**, 1134 (2011).
 - [5] V. Mendez and A. Iomin, Comb-like models for transport along spiny dendrites, *Chaos Solitons Fractals* **53**, 46 (2013).
 - [6] O. Benichou, P. Illien, G. Oshanin, A. Sarracino, and R. Voituriez, Diffusion and Subdiffusion of Interacting Particles on Comblike Structures, *Phys. Rev. Lett.* **115**, 220601 (2015).
 - [7] E. Baskin and A. Iomin, Superdiffusion on a Comb Structure, *Phys. Rev. Lett.* **93**, 120603 (2004).
 - [8] V. Arkhincheev and E. Baskin, Anomalous diffusion and drift in a comb model of percolation clusters, *Sov. Phys. JETP* **73**, 161 (1991).
 - [9] A. Dzhanoev and I. Sokolov, The effect of the junction model on the anomalous diffusion in the 3D comb structure, *Chaos Solitons Fractals* **106**, 330 (2017).
 - [10] O. Dvoretzskaya and P. Kondratenko, Anomalous transport regimes and asymptotic concentration distributions in the presence of advection and diffusion on a comb structure, *Phys. Rev. E* **79**, 041128 (2009).
 - [11] T. Sandev, A. Iomin, and H. Kantz, Fractional diffusion on a fractal grid comb, *Phys. Rev. E* **91**, 032108 (2015).
 - [12] S. Elwakil, M. Zahran, and E. Abulwafa, Fractional (space-time) diffusion equation on comb-like model, *Chaos Solitons Fractals* **20**, 1113 (2004).
 - [13] A. Iomin, Subdiffusion on a fractal comb, *Phys. Rev. E* **83**, 052106 (2011).
 - [14] V. Arkhincheev, Random walks on the comb model and its generalizations, *Chaos* **17**, 043102 (2007).
 - [15] H. Ribeiro, A. Tateishi, L. Alves, R. Zola, and E. Lenzi, Investigating the interplay between mechanisms of anomalous diffusion via fractional Brownian walks on a comb-like structure, *New J. Phys.* **16**, 093050 (2014).
 - [16] G. H. Weiss and S. Havlin, Some properties of a random walk on a comb structure, *Phys. A (Amsterdam, Neth.)* **134**, 474 (1986).
 - [17] A. Iomin, Continuous time random walk and migration-proliferation dichotomy of brain cancer, *Biophys. Rev. Lett.* **10**, 37 (2015).
 - [18] F. Hofling and T. Franosch, Anomalous transport in the crowded world of biological cells, *Rep. Prog. Phys.* **76**, 046602 (2013).
 - [19] Y. Sagi, M. Brook, I. Almog, and N. Davidson, Observation of Anomalous Diffusion and Fractional Self-Similarity in One Dimension, *Phys. Rev. Lett.* **108**, 093002 (2012).
 - [20] T. Sandev, A. Schulz, H. Kantz, and A. Iomin, Heterogeneous diffusion in comb and fractal grid structures, *Chaos Solitons Fractals* **114**, 551 (2018).
 - [21] A. Iomin and V. Mendez, Reaction-subdiffusion front propagation in a comblike model of spiny dendrites, *Phys. Rev. E* **88**, 012706 (2013).

- [22] T. Sandev, A. Iomin, H. Kantz, R. Metzler, and A. Chechkin, Comb model with slow and ultraslow diffusion, *Math. Modell. Nat. Phenom.* **11**, 18 (2016).
- [23] A. Iomin and V. Mendez, Does ultra-slow diffusion survive in a three dimensional cylindrical comb? *Chaos Solitons Fractals* **82**, 142 (2016).
- [24] G. Forte, R. Burioni, F. Cecconi, and A. Vulpiani, Anomalous diffusion and response in branched systems: a simple analysis, *J. Phys.: Condens. Matter* **25**, 465106 (2013).
- [25] I. Eliazar and J. Klafter, On the generation of anomalous and ultraslow diffusion, *J. Phys. A: Math. Theor.* **44**, 405006 (2011).
- [26] L. P. Sanders, M. A. Lomholt, L. Lizana, K. Fogelmark, R. Metzler, and T. Ambjornsson, Severe slowing-down and universality of the dynamics in disordered interacting many-body systems: ageing and ultraslow diffusion, *New J. Phys.* **16**, 113050 (2014).
- [27] Y. Liang, S. Wang, W. Chen, Z. Zhou, and R. Magin, A survey of models of ultraslow diffusion in heterogeneous materials, *Appl. Mech. Rev.* **71**, 040802 (2019).
- [28] W. Chen, Y. Liang, and X. Hei, Structural derivative based on inverse Mittag-Leffler function for modeling ultraslow diffusion, *Fractional. Calculus Appl. Anal.* **19**, 1250 (2016).
- [29] R. Gorenflo, J. Loutchko, and Y. Luchko, Computation of the Mittag-Leffler function $E_{\alpha,\beta}(z)$ and its derivatives, *Fractional Calculus Appl. Anal.* **5**, 491 (2002).
- [30] Y. Liang and W. Chen, A non-local structural derivative model for characterization of ultraslow diffusion in dense colloids, *Commun. Nonlinear Sci.* **56**, 131 (2018).
- [31] M. Caputo and M. Fabrizio, A new definition of fractional derivative without singular kernel, *Prog. Fractional Differ. Appl.* **2**, 73 (2015).
- [32] J. Singh, D. Kumar, and D. Baleanu, On the analysis of chemical kinetics system pertaining to a fractional derivative with Mittag-Leffler type kernel, *Chaos* **27**, 103113 (2017).
- [33] E. Lenzi, L. Silva, T. Sandev, and R. Zola, Solutions for a fractional diffusion equation in heterogeneous media, *J. Stat. Mech.* (2019) 033205.
- [34] W. Xu, Y. Liang, and W. Chen, A spatial structural derivative model for the characterization of superfast diffusion/dispersion in porous media, *Int. J. Heat Mass Transfer* **139**, 39 (2019).
- [35] D. Hu, W. Chen, and Y. Liang, Inverse Mittag-Leffler stability of structural derivative nonlinear dynamical systems, *Chaos Solitons Fractals* **123**, 304 (2019).
- [36] X. Yang, Y. Liang, and W. Chen, A local structural derivative PDE model for ultraslow creep, *Comput. Math. Appl.* **76**, 1713 (2018).
- [37] Y. Liang, W. Chen, W. Xu, and H. Sun, Distributed order Hausdorff derivative diffusion model to characterize non-Fickian diffusion in porous media, *Commun. Nonlinear Sci.* **70**, 384 (2019).
- [38] T. Sandev, A. Iomin, and V. Mendez, Levy processes on a generalized fractal comb, *J. Phys. A: Math. Theor.* **49**, 355001 (2016).
- [39] A. Iomin, V. Mendez, and W. Horsthemke, *Fractional Dynamics in Comb-like Structures* (World Scientific, Singapore, 2018).
- [40] B. I. Henry, T. A. M. Langlands, and S. L. Wearne, Anomalous diffusion with linear reaction dynamics: From continuous time random walks to fractional reaction-diffusion equations, *Phys. Rev. E* **74**, 031116 (2006).
- [41] R. Garra and R. Garrappa, The Prabhakar or three parameter Mittag-Leffler function: Theory and application, *Commun. Nonlinear Sci.* **56**, 314 (2018).
- [42] A. Lapolla and A. Godec, Manifestations of projection-induced memory: General theory and the tilted single file, *Front. Phys.* **7**, 182 (2019).